Environment Canada | Environnement Canada

SCIENTIFIC SERIES NO. 83
(Résumé en français)

INLAND WATERS DIRECTORATE,
CANADA CENTRE FOR INLAND WATERS,
BURLINGTON, ONTARIO, 1978.

Environment Canada Environnement Canada

Turbulent Diffusion Processes in the Great Lakes

C.R. Murthy and K.C. Miners

SCIENTIFIC SERIES NO. 83
(Résumé en français)

INLAND WATERS DIRECTORATE,
CANADA CENTRE FOR INLAND WATERS,
BURLINGTON, ONTARIO, 1978.

Cat. No. EM 36-502/83
ISBN 0-662-01888-5
Contract No. KL229-7-1040
THORN PRESS LIMITED

Contents

Tables

Illustrations

Illustrations (cont.)

Abstract

Detailed descriptions of the instrumentation, field equipment, experimental design and procedure widely used for conducting large-scale diffusion experiments in natural bodies of water such as the oceans and the Great Lakes are presented. The data analysis methods of continuous dye plume and instantaneous dye patch diffusion experiments are also given. Experimental data obtained in widely varying environmental conditions are interpreted statistically by constructing diffusion characteristics based on a simple theoretical framework.

Résumé

Les auteurs décrivent en détail l'appareillage, le matériel de campagne et la méthode expérimentale qu'ils ont utilisés pour réaliser leurs expériences de diffusion à grande échelle dans les étendues naturelles d'eau comme les océans et les Grands lacs. Ils décrivent aussi les méthodes d'analyse des données utilisées dans les expériences de diffusion des traînées de colorant obtenues par lâchage continu et des taches de colorant obtenues par lâchages ponctuels. Ils interprètent statistiquement les données expérimentales recueillies dans des milieux très variés en traçant les caractéristiques de diffusion, définies à partir d'un appareil théorique relativement simple.

Introduction

The circulation in natural bodies of water such as the Great Lakes generally consists of very complex turbulent motions. Superimposed on the mean flow circulation patterns are eddy-like motions of varying intensity and scales. These eddy-like motions exist in both horizontal and vertical directions. The scale of horizontal eddies, however, is much larger than the scale of vertical eddies because the lakes are many times wider than they are deep. A direct consequence of this is the large-scale water movements and the associated transport and dispersion of chemical and biological species from one area of the lake to another. The practice of discharging municipal and industrial wastes including waste heat from thermonuclear power plants provided impetus for extensive theoretical and experimental studies of turbulent diffusion processes in natural bodies of water. However, turbulent diffusion processes are complex, and theoretical predictions of transport and dispersion of these wastes are far from satisfactory. Thus, an understanding of the various manifestations of turbulent diffusion processes is largely dependent on the empirical approach of conducting field diffusion experiments. In this report we will discuss in some detail the instrumentation, field equipment, experimental network and procedure widely used for conducting large-scale diffusion experiments. The data analysis and interpretation of experimental results of continuous dye plume and instantaneous dye patch diffusion experiments are also presented.

Fluorometric Technique

FLUORESCENCE

Fluorescence is a physical phenomenon; it is the instantaneous emission of light from a molecule or atom that has absorbed light. It is a type of radiant energy emission that is produced when a substance returns to a normal state after having been raised to an excited condition by the absorption of energy. One of the first substances observed to produce a visual radiation after it had been excited by a high-energy source was the mineral fluorspar, and hence, the term "fluorescence". If the emission persists over 10^{-8} to 10^{-9} s after the exciting source is removed, the phenomenon is called "phosphorescence", sometimes loosely called "delayed" fluorescence. The exciting source and the emission may be in any part of the spectrum.

Turning to fluorescence in general, in the brief period of 10^{-8} to 10^{-9} s before the emission can occur, some energy is lost, so the emitted light (fluorescent light) is of longer wavelength than the light that was absorbed (exciting light). For example, if ultraviolet (UV) light is absorbed, the emission may be in the longer wavelengths, UV, blue, green, yellow or red region of the spectrum. If blue light is absorbed, the material may fluoresce in green, yellow or red, etc.

Fluorescence, therefore, is essentially an electronic phenomenon and is primarily concerned with the light of wavelengths in the region of 200 to 800 nm. Some compounds when illuminated with light of this region only absorb specific wavelengths of this light and the wavelengths absorbed are characteristic of the particular compound being examined. The extent to which the light of these wavelengths is absorbed constitutes the absorption spectrum of the compound. As a consequence of the absorption of light, some of the molecules of the compound become excited because certain electrons in the molecule are raised to a higher energy level. This is shown diagrammatically in Figure 1 by horizontal lines and the directions of the energy transitions are shown by vertical and inclined arrows. On absorption of light, the molecule is raised from the ground state G to the excited state E, as indicated by the vertical arrow A. The molecule returns to the ground state, emitting some of its absorbed energy as fluorescence, as indicated by the arrow marked F. An electronic transition due to light absorption is almost instantaneous (10^{-15} s), whereas the lifetime of the excited state is about 10^{-8} s and, therefore, the whole process of light absorption and fluorescence emission takes place in about 10^{-8} s. Now some of the energy absorbed is lost partly by collisions with other molecules and partly by other means, so that less energy is emitted as fluorescence than was absorbed from the exciting light. According to the quantum theory, light is absorbed in discrete units called quanta and the energy (E) of a quantum is related to vibrational frequency (γ), thus $E = h\gamma$, where h = Planck's constant. Frequency is related to wavelength (λ) according to the expression, $\gamma = c/\lambda$, where c is the velocity of light. From these two equations, $E = hc/\lambda$, and, since h and c are constants, E varies inversely as λ. As mentioned above, the energy emitted as fluorescence is less than the light energy absorbed and, therefore, from the last equation, the wavelength of fluorescence is longer than that of the absorbed light.

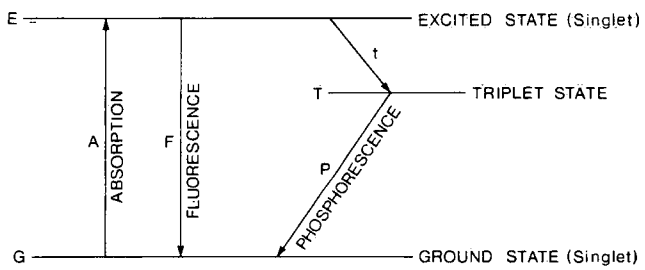

Figure 1. Energy levels, absorption, fluorescence, and phosphorescence.

The mechanism of phosphorescence is also illustrated in Figure 1. This phenomenon is distinguished from fluorescence by the much longer lifetime of the excited state (which may be up to several seconds). To understand the reason for this difference, one must consider the spin of the electrons of a molecule. Electrons in most molecules are found in even numbers and are paired. In each pair, the two electrons spin about their own axis in opposite directions (anti-parallel spins) and for reasons which need not be considered here, such molecules are said to have a "singlet" electronic level. When the molecule is raised to the excited state, two things could happen: (1) the electrons may remain "singlet" and the molecule can then return to the ground state with the

emission of fluorescence (path F), or (2) one electron, by some internal energy transition, may have its spin reversed (parallel spins) and the molecule is then said to have a ''triplet'' electronic level.

In Figure 1, this change is indicated by the top inclined arrow t, and the ''triplet'' excited state is indicated by the horizontal line T. Such a molecule is regarded to be in a metastable state. The lifetime of the triplet excited state is longer than that of a singlet excited state, for the molecule has to return to the ground singlet state by what is known as a ''forbidden transition'', which has a low probability. During this return, there is emission of phosphorescence, as indicated by the inclined arrow P. In the transition from the singlet excited state to the triplet state, there is loss of energy, for the energy level T is lower than E. Therefore, there is less energy emitted in the transition from T to G, so that the wavelength of phosphorescence is longer than the wavelength of the fluorescence that would have been produced by the same excitation. Fluorescence is thus an emission from a singlet excited state (electron spin paired), whereas phosphorescence is emission from a triplet excited state (electrons unpaired). Phosphorescence persists longer than fluorescence and this persistence is prolonged and the intensity enhanced by low temperatures.

With this fundamental concept, let us consider how we can use fluorescence technique for water tracing problems. Any given fluorescent molecule in a given environment has two characteristic spectra: the excitation spectrum (the relative efficiency of different exciting wavelengths to cause fluorescence) and the emission spectrum (the relative intensity of light emitted at various wavelengths). Each molecule also has a characteristic quantum efficiency, which is the ratio of total emitted light to total absorbed light.

FLUOROMETRY

Fluorometry is the measurement and use of fluorescence. In the filter fluorometer, which is easy to use, the wavelengths of exciting light and emitted light are selected by coloured filters. The desired wavelengths of exciting light are selected by a filter (called the primary filter) between the light source and the sample. The wavelengths of light to be measured are selected by a second optical filter (called the secondary filter) between the sample and photo-detector. The output of the photo-detector, a current which is proportional to the intensity of the fluorescent light, is amplified to give a reading on a meter or a recorder. In a spectrofluorometer, the filters would be replaced by infinitely variable monochrometers and an x-y recorder would be used, displayed wavelengths as well as fluorescence.

A filter fluorometer measures the ratio of the intensities of the fluorescent light and a constant proportion of the light from the light source (see Fig. 2 for details). A fluorometer is an optical bridge which is analogous to the accurate Wheatstone Bridge used in measuring electrical resistance. The optical bridge detects the difference between light emitted by the sample (fluorescent light) and that from a rear light path. A single photomultiplier surrounded by a mechanical light interrupter sees light alternately from the sample and the rear light. Path photomultiplier output is alternating current, permitting a drift-free AC amplifier to be used for the first electronic stages. The second stage is a phase-sensitive detector whose output is either *positive* or *negative*, depending on whether there is an excess of light in the *sample* or rear light path, respectively. Output of the phase detector drives a servo-amplifier, which is, in turn, connected to a servo-motor. The servo-motor drives the light cam (and the fluorescence dial) until equal amounts of light reach the photomultiplier from the sample and from the rear light path. The quantity of light required in the rear light path to balance that from the sample is indicated by the fluorescence dial. Each of this dial's 100 divisions adds equal increments of light to the rear light path by means of the light cam.

FLUORESCENCE INTENSITY AS RELATED TO CONCENTRATION

A filter fluorometer is an instrument which gives a relative measure of the intensity of light emitted by a sample containing a fluorescent substance. The intensity of fluorescent light is proportional to the amount of fluorescent substance present. However, a fluorometer reading by itself has little meaning until it is compared with readings for samples of known concentrations on the same fluorometer under the same instrumental and environmental conditions.

The fluorescence intensity of dilute solutions is a straight-line function of concentration.

The application of the Lambert-Bouguer-Beer law to fluorescence may be formulated as follows. From the absorption law:

$$I/I_0 = 10^{-\varepsilon cd} = \text{fraction of light transmitted}$$

where I = the intensity transmitted; I_0 = the incident

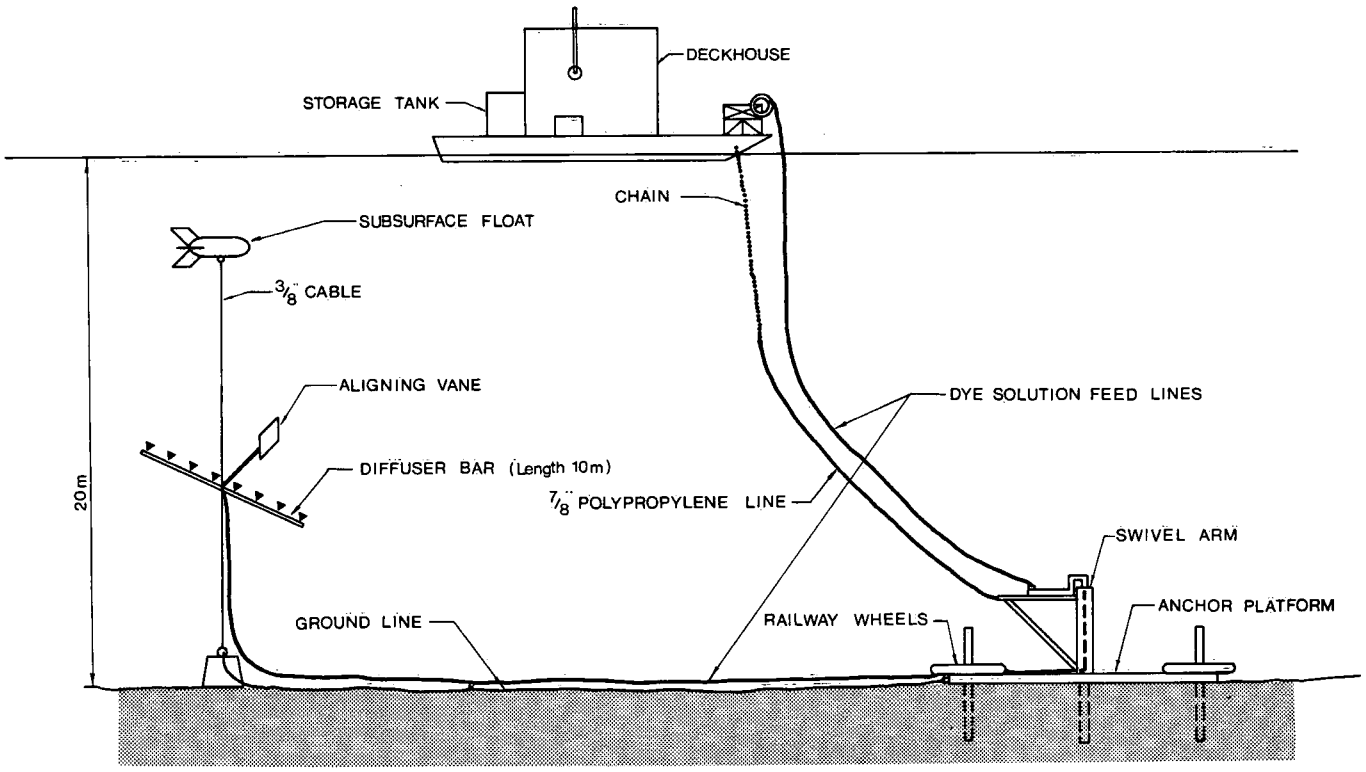

Figure 2. Continuous dye release system.

intensity; e = the molar extinction coefficient; c = the concentration; d = the cell thickness.

Fraction of light absorbed:

$$1 - I/I_0 = 1 - 10^{-ecd}$$

$$I_0 - I = I_0(1 - 10^{-ecd}) = \text{amount of light absorbed.}$$

The intensity of the fluorescence is proportional to the amount of light absorbed:

$$F = K_1 I_0 (1 - 10^{-ecd}).$$

By expansion of the term in the parenthesis

$$F = K I_0 \left[2.3\ ecd - \left(\frac{-2.3\ ecd}{2}\right)^2 - \left(\frac{2.3\ ecd}{3}\right)^3 \ldots\ldots - \left(\frac{2.3\ ecd}{n}\right)^n\right]$$

If ecd is small, the latter terms can be dropped and

$$F = K I_0\, 2.3\, ecd$$

or, since e and d are constants for one cell, and one compound and the light source may be kept constant,

$$F = k c.$$

The straight-line relationship is the one commonly used.

FLUORESCENT TRACERS

Some essential properties of tracer dyes for water tracing problems are water soluble, highly detectable by their fluorescence, harmless in low concentrations, inexpensive, and reasonably stable in natural surface water movement and environment. Some dyes commonly used are Fluorescein, Rhodamine B, and Pontacyl Brilliant Pink B. Other dyes specifically developed for water tracing needs are Rhodamine BA and Rhodamine WT.

Rhodamine B, a commercial organic pigment used in lipstick and children's pink birthday candles, is an excellent tracer material in that it fulfils the above characteristics adequately. It is non-toxic to human beings and fish can survive for at least 2 months in 100-ppm solutions. It is quite soluble in water and is usually available commercially in 30 or 40 per cent by weight

solution in acetic acid. Adjustment of the specific gravity is necessary, since solutions are heavy in these concentrations. It is highly soluble in methanol, so that concentrated solutions may be adjusted to the same density as that of the receiving waters, to prevent undesirable settling or stratification in the receiving bodies of water.

For oceanographic work, solutions are available at the specific gravity of sea water, approximately 1.03. For most freshwater tracing, 1.03 is low enough. Rhodamine B solutions with specific gravities ranging from 1.00 to 1.09 are available. However, Rhodamine B solutions with specific gravities of 1.00 to 1.03 are recommended for most water tracing problems such as time of travel of streams, groundwater movement (hydrology) and dispersion studies, primarily because of the cost factor. Other dyes (although superior in some respects) are not economical for large-scale use.

Rhodamine B dye is readily detected by its fluorescence. The absorption spectrum of this dye has a maximum at 550 nm so that the molecule is strongly excited to fluoresce by the green (546 nm) line of mercury. The green mercury line may be isolated by simple optical filters, so that the nearly monochromatic exciting light is easily filtered from the emitted path and the effects of scattering are almost completely eliminated. The fluorescence spectrum of Rhodamine B has a maximum at 575 nm. Figure 3 shows the excitation and emission spectra for Rhodamine B dye solution (0.1 mg/ml) when excited by the 546-nm line of a xenon lamp. The principal component of fluorescence background might be expected to be chlorophyll and its derivatives. The Rhodamine B light is easily separated from that of plant pigments, which occurs from 650 to 700 nm.

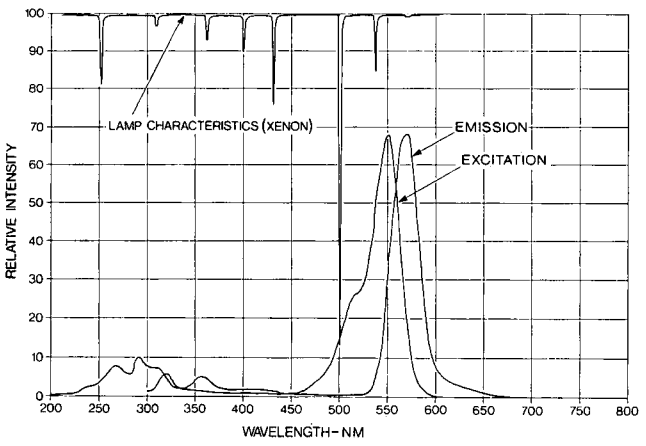

Figure 3. Excitation and emission spectra for Rhodamine B.

Rhodamine B (WT) and Pontacyl Brilliant Pink (or equivalent) have nearly the same spectral properties, making them all highly detectable with the 546-nm and 590-nm filter fluorometer. Selection of the proper filters is very important in fluorescence measurements. Some of the essential considerations in filter selection for a particular fluorescent dye are the excitation and emission spectra of the particular dye used; the useful output spectrum of the exciting lamp; potential interference from fluorescence of background materials (background fluorescence); and potential interference from light scattered in the water sample.

A particular new dye may require an entirely different set of filters from that used for Rhodamine B. Failure to recognize and determine this in advance may result in false conclusions about the detectability or even the presence of the dye.

The fluorometer could detect Rhodamine dye concentrations as low as 2×10^{-10}. With the use of ND filters, concentrations up to 2×10^{-7} could be measured. Above this concentration, the solutions started to become opaque to the exciting light ("quenching").

Calibration of the fluorometer should be made with in situ water in the fields with temperatures kept constant. The procedure to calibrate Turner model III fluorometer is described in the Appendix and typical calibration curves are shown in Figure 4.

RADIOACTIVE TRACERS

The use of radioactive tracers for water movement studies in large bodies of water such as lakes, although restricted at the present time, is no doubt a potentially useful technique for future studies. Evaluation of eddy diffusivities from the dispersal of dye introduced into the lake is highly laborious and expensive, and involves frequent sampling of dye concentrations. Radioactive tracer sources and the detectors are relatively inexpensive compared with a conventional dye source and instruments currently employed. Dilution and residence time studies of the effluents discharged into receiving waters have been successfully carried out in certain European waterways using radioactive bromine-82.

Radioactive nuclide ^{212}Pb has been suggested as one of the possible tracers for diffusion studies in lakes. Its half-life is only 10 hr, rather too low for time scales encountered in the Great Lakes. Radioactive ^{82}Br (half-life 36 hr) has been used by Cederwall and Hansen (1968) in Swedish Waterway Investigations. The choice of a

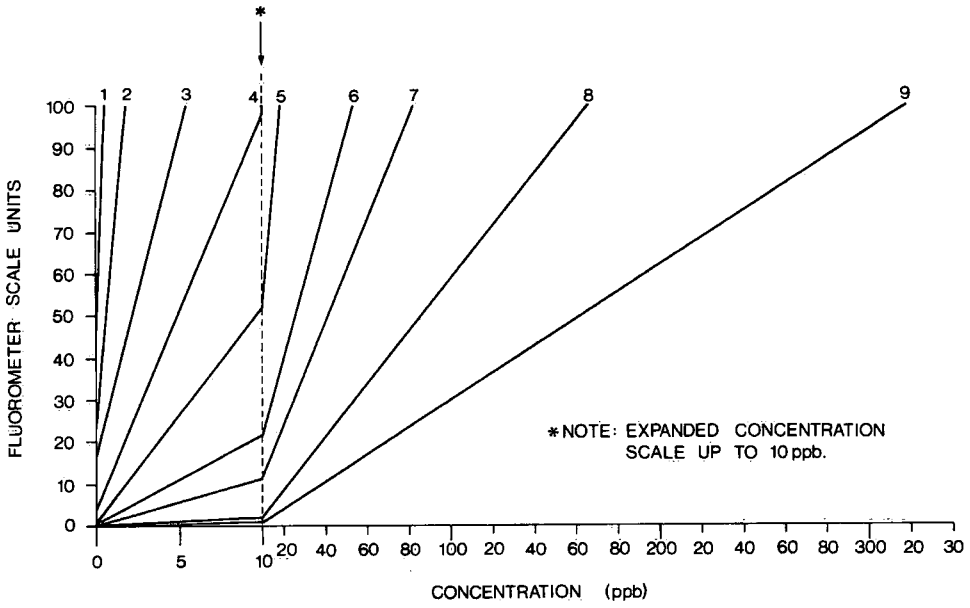

CURVE NUMBER	NO. OF N.D. FILTERS 50%	10%
1	0	0
2	1	0
3	2	0
4	0	1
5	1	1
6	2	1
7	0	2
8	1	2
9	2	2

Figure 4. Typical calibration curves for Turner model III fluorometer.

radioactive tracer for Great Lakes diffusion studies is critical. Some desirable characteristics are the following.

(a) Half-life should be comparable to the time scales of the Great Lakes diffusion processes. A tracer with a half-life of about 5-10 days is rather ideal to replace the currently popular fluorescent tracers. (Half-lives of some of the fluorescent tracers currently used are Rhodamine B, 65 hr; Pontacyl Brilliant Pink, 460 hr.)

(b) Produces no radiation hazards.

(c) Decay through short half-lives to stable and easily detectable end product.

The radioactive nuclide ^{212}Pb has the following characteristics that indicate that it may be highly useful in the measurements of eddy diffusivity.

(a) ^{212}Pb has been successfully used in the studies of atmospheric turbulence.

(b) Its half-life is 10.6 hr.

(c) It produces no radiation hazards (decays through short half-lives to the stable end product ^{208}Pb).

(d) ^{212}Pb forms from the gas ^{220}Rn, which decays to ^{212}Pb with a half-life of 56 s. ^{220}Rn is one of the intermediate products of the decay of ^{228}Th (half-life 1.9 years).

(e) ^{228}Th source, releasing the gas ^{220}Rn into the water, is the primary source of ^{212}Pb, the dispersal of which is to be measured. ^{228}Th sources are inexpensive.

The method of measurement—With a ^{228}Th source immersed in the lake, the equilibrium activity of ^{212}Pb can be recorded at different distances from the source. ^{212}Pb has a strong gamma line at 2.61 meV, which is virtually free of natural background. Measurements can be done with one NaI crystal, moving it at certain time intervals to different positions relative to the source (three detectors would, of course, make the procedure more rapid).

Some calculations have been made on the suitability of ^{212}Pb for eddy diffusion measurements in lakes and ocean: its half-life is just right for the magnitude of eddy diffusivity in lakes.

Keeping a ^{228}Th source for up to a few days in a lake should be, in principle, possible. One difficulty may arise: the first daughter of ^{228}Th is ^{224}Ra; the latter decays to ^{220}Rn, which should diffuse into the water. However, radium, being more soluble than thorium, might also escape from the source into the lake water. If this happens, additional ^{212}Pb would be generated in the water. Such a process would either have to be corrected for in the calculation, or ^{224}Ra would have to be prevented from escaping from the source. Air or inert gas blown at a slight pressure differential over the source should remove ^{220}Rn from it and transfer it by slow bubbling at a controlled rate into the lake water. ^{224}Ra would remain on the source, which would not be in contact with the lake water.

The length of time it would take to have the method work depends greatly on the facilities available: ^{228}Th source would have to be purchased (probably custom designed); a machinist and an electronics technician and/or engineer would have to be employed during different stages of the assembling and testing of the equipment; the basic components of the gamma counting assembly and NaI detector for underwater work can be purchased from manufacturers.

Dye Release and Sampling Techniques

DYE RELEASE SYSTEMS

Continuous Release

A 3 × 8 m catamaran with a 2 × 3 m deckhouse served as a surface platform for the dye injection system with ample reserve space for storage of service equipment and spare parts. A 3 kW (110 V, 60 Hz) air-cooled diesel generator supplied the necessary power for the injection system with plenty to spare for lighting and other auxiliary equipment.

The dye release system was designed for uninterrupted, accurate delivery of dye solution for periods of up to several days. Figure 5 is a schematic diagram of the dye injection system used in Great Lakes diffusion studies. The dye solution delivered through the main feeder hose was the combined output of two subsystems: a high-pressure, low-volume injecting system which metered the dye from the storage tank; and a low-pressure, high-volume water pumping system. The main and auxiliary metering pumps were capable of accurate metering of dye solution over a precisely adjustable range of 0 to 64 l/hr, to inject dye into the feed line. A submersible well pump was employed to supply water to the feed line.

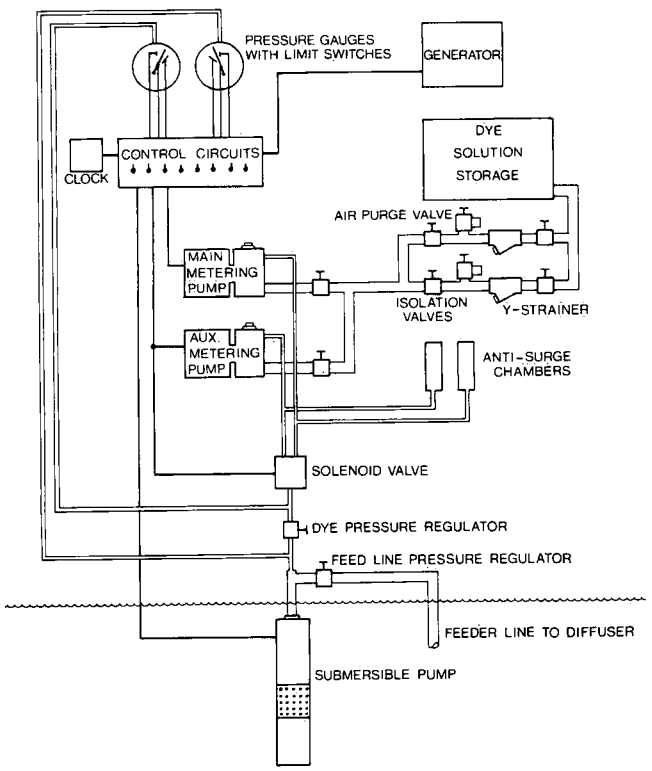

Figure 5. Injection system, schematic.

A control circuit consisting of four double pole-double throw (DPDT) relays, a timed relay, and two pressure gauges equipped with adjustable high- and low-pressure-limit switches, continually monitored the operation of the injection system. Normally, the pressure of the metering pump outlet was kept above feed-line pressure by a needle valve. Failure of the metering pump would allow the pressure to fall to feed-line pressure, which would close the low-pressure-limit switch on the gauge monitoring that part of the system. This, in turn, would result in shut-down of the main pump and simultaneous start-up of the auxiliary pump. A three-way solenoid valve on line with the auxiliary pump opened to flow from the auxiliary and closed to flow in the main pump outlet, thereby preventing back-flow into the main pump if the failure were due to faulty valves or ruptured diaphragm. Low pressure conditions also activated the timed relay. If auxiliary start-up failed to restore operating pressure within 15 s, the entire system would shut down. High pressure conditions immediately shut down the entire system on the assumption that switching to auxiliary would not alleviate the fault.

Indicator lights on the control panel remained lit upon failure to show what component had failed and whether pressure had gone too high or too low; and a 24-hr digital clock stopped with the system to indicate time of failure. These features aided trouble-shooting immensely.

System failures nearly always originated in the dye-metering network. The metering pumps were very reliable but at such low flow rates a very small amount of sludge or gas would halt flow. These contaminants were minimized by the installation of fine strainers and vapour traps on the pump inlets. In addition, the stock 40% dye solution was further diluted in the tank by addition of methanol in the ratio of 1 part to 2 parts dye. This redissolved most sludge present and also allowed a

higher flow rate to be used without net increase in dye concentration. The solution in the tank had a concentration of 27% rhodamine by weight and was pumped at a rate of 12 l/hr. When the solution was mixed with water in the feed line, the concentration dropped to 2.35×10^{-3} with a total flow rate of 1370 l/hr.

Figure 6 shows schematically the dye release system used for continuous release experiments. The dye release system was designed to simulate, on a small scale, point source pilot dye plumes or line source dye plumes at any depth ranging from 3 to 20 m mostly in coastal waters of the Great Lakes. On occasions, the dye release system was used successfully to generate line source dye plumes 3 m off the lake floor about 1 - 1½ km offshore to simulate the discharge of waste effluents through multi-port submarine diffusers commonly used by many municipal and industrial coastal sites.

Whereas an actual system would be fixed, the simulator was made to rotate such that the tail fin would keep the bar perpendicular to the flow, with the nozzles pointing downstream. This was done so that the plume width at source would not be a function of the diffuser's attitude to the flow. Dye solution entered the hollow centre-link of the diffuser bar through a free-rotating,

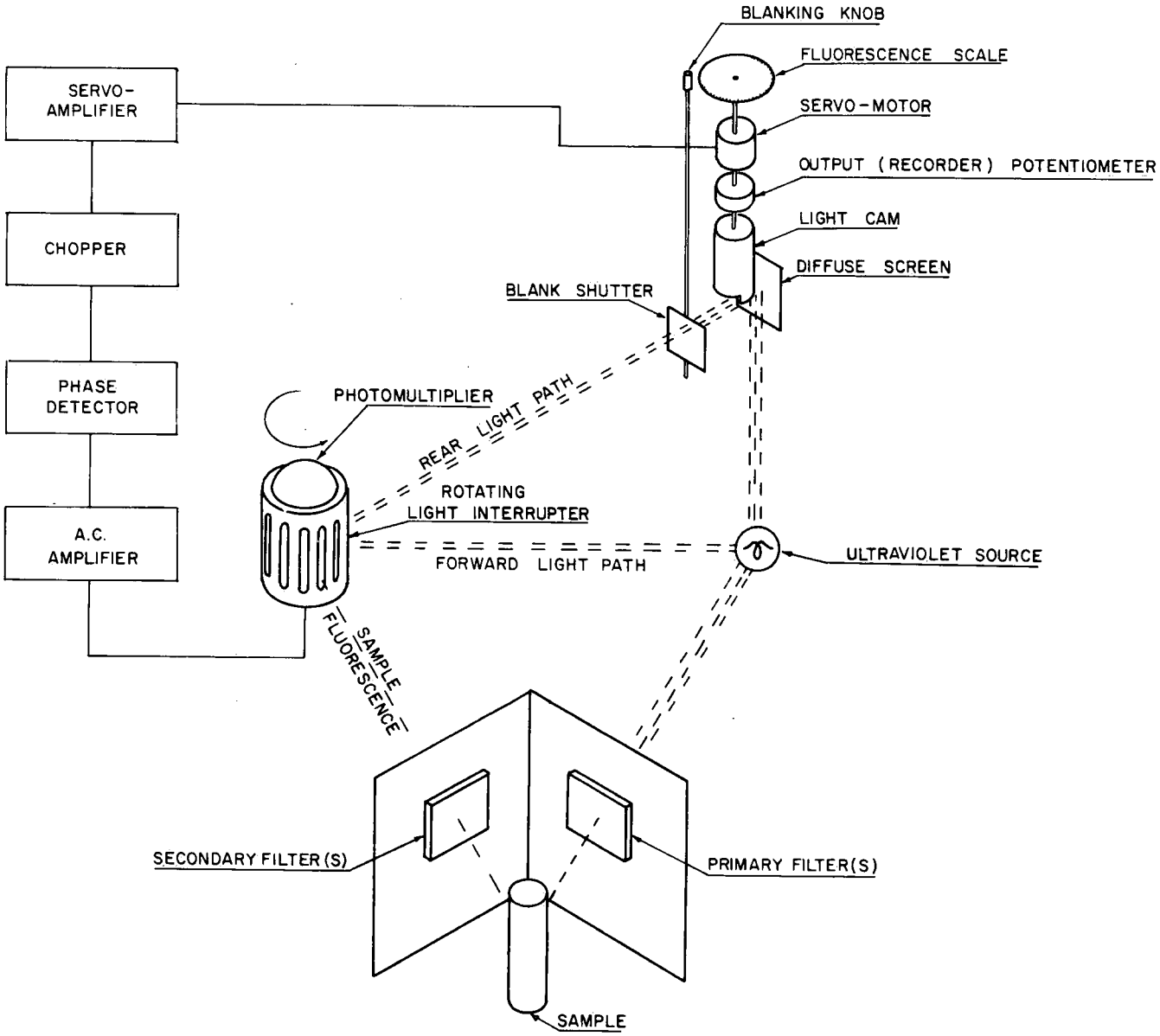

Figure 6. Turner fluorometer, optical system and major electronic stages.

'O'-ring-sealed coupling. It then flowed out into the arms of the device, which were constructed of 5-m lengths of 38-mm stainless steel pipe. From here, the dye entered the water through the ten 1.6-mm-diameter nozzles mounted at 1-m intervals along the length of the bar.

The solution to the problem of mooring the source in the open lake for several months would have been fairly simple had it not been necessary for the feeder hose to run from the platform to the diffuser. Exposure to bad weather ruled out anchoring the platform from four corners, which would have simplified the feeder hose installation; and mooring on a single line with sufficient scope to allow the platform to ride out heavy seas head-on would have provided endless opportunity for the hose to foul on the anchor, boulders on the bottom, etc., if it were simply laid out from the deck to the diffuser mooring. Many of the difficulties were eliminated with a unique anchor consisting of a 2-m-square steel platform with a 17-cm-diameter steel leg extending above and below the platform at each corner and in the centre. A rugged triangular frame was secured to the taller centre leg with two steel rings which allowed the frame to rotate about the leg. The mooring line from the injection platform was attached to the outer corner of the frame, while the feeder hose attached to a pipe running along the top of the frame to a rotating union in the centre of a top cap on the leg. From the bottom fitting of the union, a hose ran down the inside of the leg and out to one corner of the anchor. From here a final length of hose ran across the lake bottom and up to the diffuser some 60 m away, well outside the scope of the moored platform.

Anchor line lengths at least five times the water depth are desirable; however, the feeder hose and anchor line for this application were only about twice the water depth, to reduce the opportunities for fouling. Additional measures were taken to keep the lines off the bottom, and below the platform, even when maximum slack developed with the platform drifting over the anchor—a situation which was observed with surprising frequency. At the platform end, the anchor line was made up of 15 m of 9.5-mm chain; the rest was 25 m of 22-mm floating polypropylene rope. The feeder hose was 13-mm nylon-reinforced vinyl garden hose, buoyed up over the lower 15 m with styrofoam rings. At the platform, the hose entered the water from a reel mounted on the starboard rail near the bow. Several metres of extra hose were wound on the reel, which was stopped off with light line such that excessive strain on the hose would part the line and free more slack hose. In spite of all precautions, the lines did foul a few times during 4 months of service; however, damage and downtime attributable to this cause were minimal.

Instantaneous Release

In our earlier experiments, the catamaran used for continuous release experiments was equipped to generate instantaneous dye patches at a fixed depth. A high-volume centrifugal pump was used to release the dye. The dye solution from the storage tank was pumped through a vertically mounted discharge pipe 4 cm in diameter extending 5 m below the surface with a diffuser section having 1.25-cm holes uniformly distributed. The diffuser pipe was supported by four cables connected to the bottom of the deck. The release time for 500 - 750 litres of dye solution was about 100 s and, thus, the dye patch could be treated as instantaneous. Figure 7 shows schematically the dye release system with diffuser section in position.

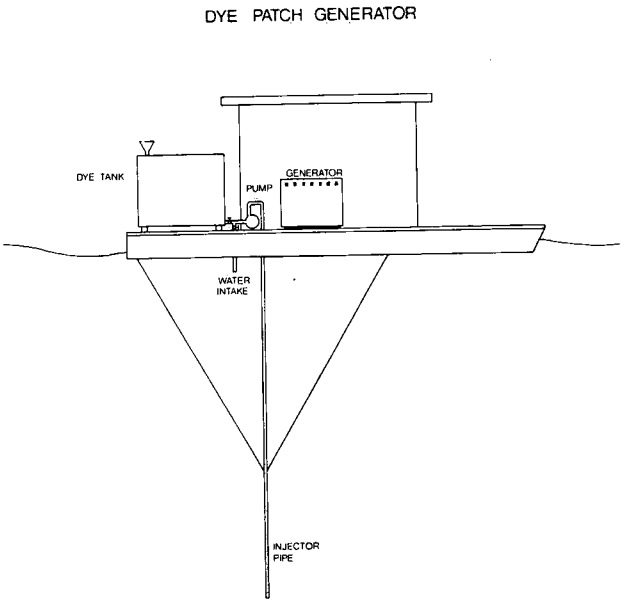

Figure 7. Instantaneous dye release system.

In our later experiments during the 1972 International Field Year for the Great Lakes, a specially built in situ instantaneous dye release system was used. The system consists of fibre glass cylinder and an aluminum end-plate assembly with a release mechanism. The in situ preparation of the dye release system consists of positioning the end-plate assembly in the cylinder and sealing it with inflated bicycle inner tubes. The entire assembly is supported by cables from a winch during preparation. The cylinder is lowered to the water and filled with dye solution via hydraulic connectors at the top. When full, the cylinder is lowered to the desired depth. A messenger weight dropped down the cable triggers the air valve to the seals. When the seals deflate sufficiently, the cylinder drops down and the dye solution

is released almost instantaneously. The dye patch thus generated is allowed to drift away from the area of release before recovering the dye release system. Figure 8 shows the dye release system and illustrates the three phases of in situ preparation for generating an instantaneous dye patch.

SAMPLING SYSTEM

Throughout our diffusion studies, Canadian Survey Launch *Aqua* served as the principal dye sampling vessel and was equipped to sample from three depths simultaneously. The continuously pumped sample from each

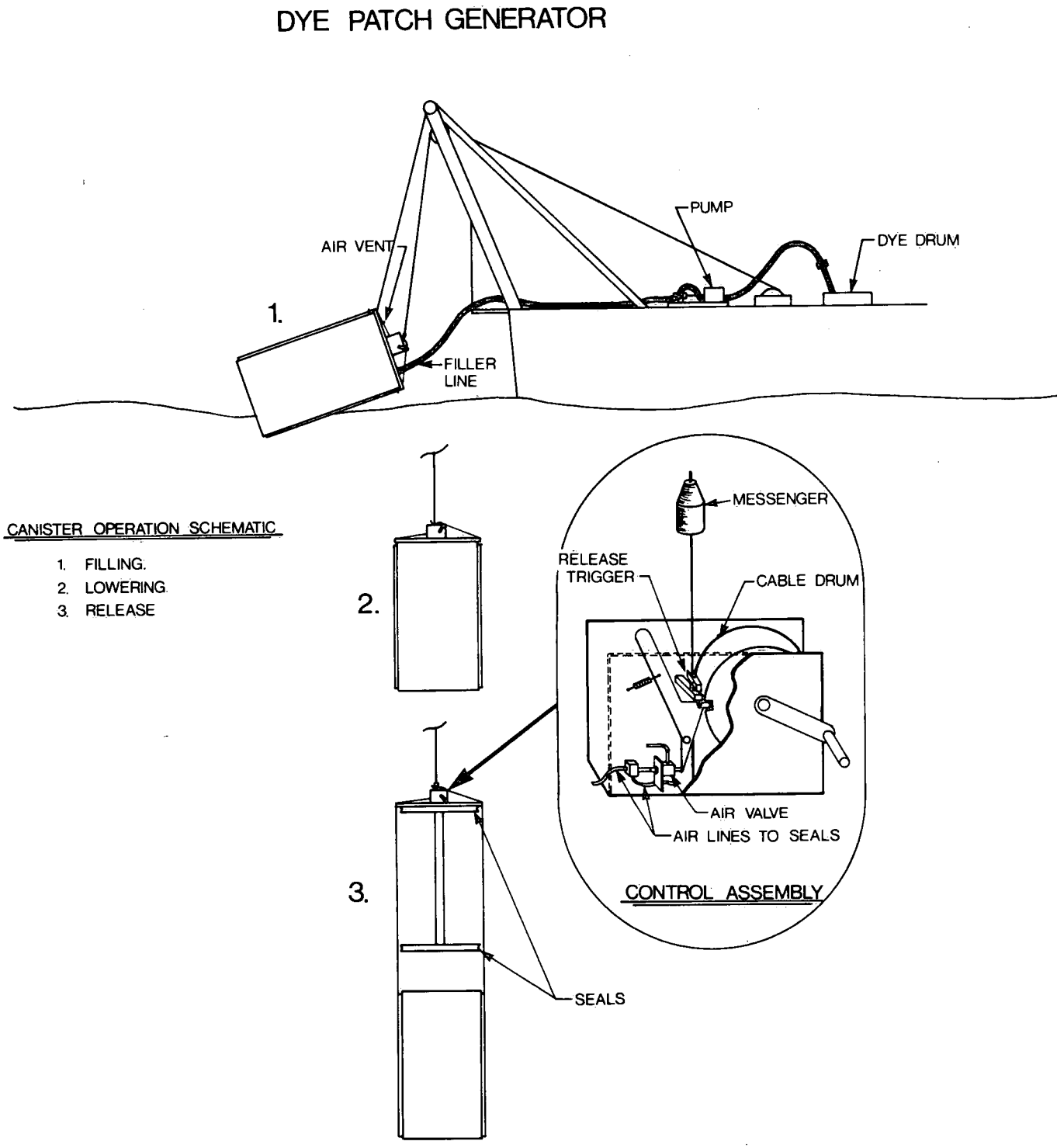

Figure 8. Instantaneous dye release system.

depth passed through a Turner model III fluorometer equipped with a high-volume flow cell. The fluorometer output, a linear function of dye concentration, was recorded on an analog recorder.

Submersible pumps were mounted at 1, 3, and 6 m on a 6-m-long, foil-shaped, extruded aluminum sailboat mast. During sampling, this boom hung vertically from a bracket on the port gunwhale of the sampling launch. A cable running from a handwinch mounted near the bow to the lower end of the boom served as a brace and a means of raising and lowering the boom. When not in use, the boom was drawn up horizontally and pulled in board.

Neoprene-covered cables supplying 110 V AC power for the pumps, and nylon-reinforced vinyl garden hose to carry the samples passed through the hollow core of the boom. The upper ends of the hoses led into the cabin and attached to the instruments. A second hose on each instrument exhausted sample waste over the side.

The system on the *Aqua* (Fig. 9) was arranged such that the portion of the sample path from the gunwhale near the top of the boom to an instrument cabinet inside the cabin consisted of permanently mounted copper pipes. The instruments were mounted on roll-out shelves in the cabinet. Each compartment had its own door, making it possible to protect the instruments from direct sunlight which might have entered the detector compartment of the instruments.

The instrument cabinet, which was built to accommodate up to six instrument systems, had a separate rack to hold analog recorders at a convenient height to monitor

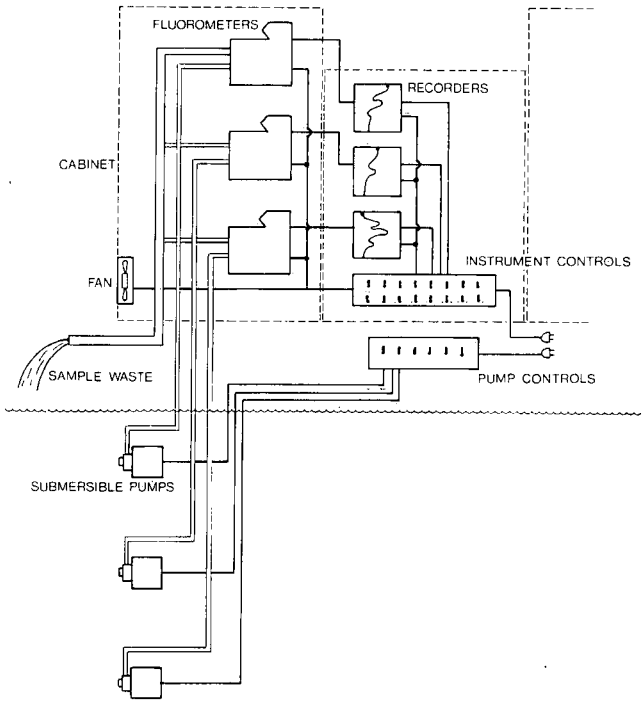

Figure 9. Sampling system, schematic.

their operation and enter handwritten information. A switch panel below the recorders provided control over instrument power in addition to individual and ganged event marker and pen-lift control. To reduce further the maze of wires and hoses, a collector manifold for sample waste was installed in the back of the cabinet, reducing the effluent to a single pipe. To prevent overheating of the confined instruments, two fans were installed in the cabinet to maintain airflow.

Coastal Zone Diffusion Studies

EXPERIMENTAL METHODS

To study turbulent diffusion processes in the coastal zones of large natural bodies of water such as the Great Lakes, pilot fluorescent dye plumes generated in the wake of a continuous release source are often convenient. They can be studied with relative ease from small boats fitted with sampling instruments. Experimental procedure generally consisted of generating a dye plume by releasing Rhodamine B dye solution at a specified depth and at a constant rate of 3.3 cm^3 s^{-1}. Continuous plume experiments were conducted in coastal waters 1 - 2 km from the shore in water depths ranging from 15 to 20 m. In a typical experiment, the dye was released in the early hours of the day and the plume thus generated due to lake currents was allowed to develop for 2 - 3 hr. The early stages of diffusion are difficult to sample since the dye plume is slender and has high concentrations beyond the measurability range of the fluorometers. Moreover, any significant disturbance of the plume by the sampling vessel would drastically alter the diffusion further downstream.

While the dye plume developed, the sampling system described earlier was prepared. The instruments were turned on for prewarming and zero-checks were made on the fluorometers and strip chart recorders by pumping ambient lake water through the sampling system. Once the dye plume was developed sufficiently, the first cross section was established at a fixed distance from the source by anchoring flag-buoys on either side of the plume such that the line joining the two flag-buoys was perpendicular to the mean plume direction. The sampling was carried out by criss-crossing the dye plume several times between the anchored flag-buoys. The positions of these flag-buoys and the dye source were established for each experiment from shore-based transit stations.

Samples were drawn at the leading edge of the boom and pumped through the fluorometers on the deck of the boat. The output signal from the fluorometers was recorded on strip chart recorders. A flow rate of approximately 70 cm^3 s^{-1} was maintained to minimize the lag time in the tubing and to obtain good response characteristics from the sampling system (typical response time of the system was 10 - 12 s). Because of the time lag between the sample intake and the fluorometer response, sampling was extended well past the visible extent of the dye plume. The extra time so taken up was sufficient for the mean current to displace the disturbed plume section before the next (return) crossing.

With a boat speed of 1 - 2 m s^{-1}, very good resolution of the spatial coordinate on the strip chart recorder was achieved. The average boat speed was determined from the distance between the anchored marker flags from the shore-based surveys and the average time taken to cross them in a number of runs. The time base of the fluorometer traces was converted to a distance scale from the average boat speed and the chart speed.

During the experiment, measurements of current velocity profiles and temperature profiles were taken at the location of the dye source.

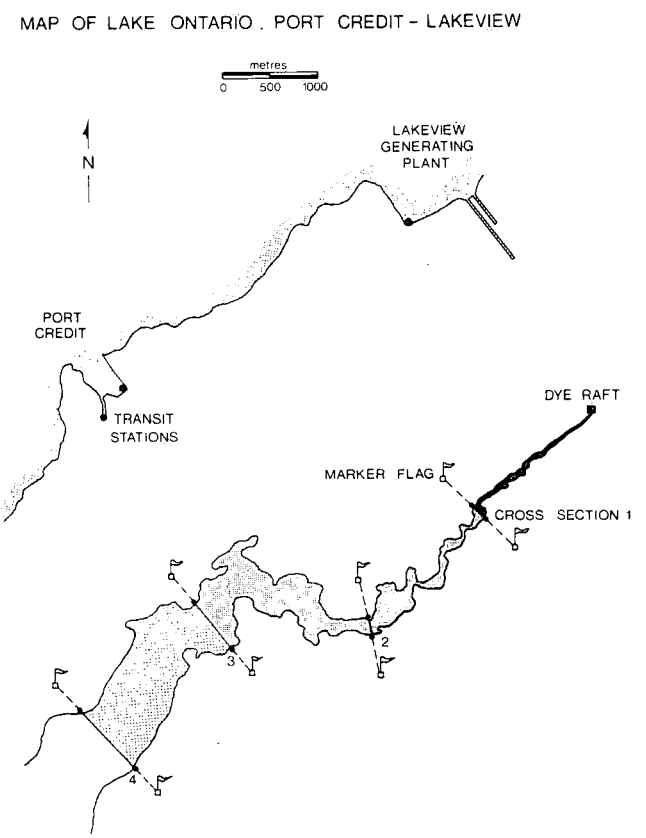

Figure 10. Continuous plume experiment, schematic.

An adequate quantitative description of the dispersal of a dye plume generated in the wake of a point source requires that concentration profiles be obtained along several equally spaced cross sections of the plume. Concentration profiles obtained simultaneously from several depths provide the basis for a reasonable reconstruction of the plume in three dimensions. Moreover, the acquisition of several sets of profiles at each cross section facilitates statistical treatment of the data and the construction of a "mean" plume free from random features, prevalent in the "instantaneous" picture derived from individual profiles.

A schematic diagram of the experimental technique is shown in Figure 10. To obtain adequate data, about 10 - 12 hr was spent on each experiment.

DATA ANALYSIS

When fluorescent dye is released continuously into turbulent coastal currents, the subsequent transport and diffusion may be studied either in a frame of reference moving with the centre of gravity of the plume or in a frame of reference fixed to the stationary source. Conventionally, the former is referred to as "relative" diffusion and the latter as "absolute" diffusion. The interlink between the two concepts is explained by the random movements of the centre of gravity of the diffusing plume usually referred to as the "meandering". Following Gifford (1959, 1960) and Csanady (1963), one may regard "absolute" diffusion (that which is measured at a fixed point) as a superposition of the two component processes of "relative" diffusion, i.e., diffusion relative to the centre of gravity of the plume and "meandering" or bodily displacements of the diffusing plume parcels.

The gross physical factors involved in the dispersal of a diffusing cloud (or a continuous plume) of marked fluid in a turbulent flow field can be elucidated reasonably well from a description of the "mean" concentration distribution. A large number of cross-plume instantaneous concentration profiles obtained at a constant depth, z, and at a fixed distance, x, from the dye source were used to construct the "absolute" and "relative" mean concentration profiles. To construct "relative" mean concentration profiles, the individual concentration profiles were overlapped such that their centres of gravity coincided. The profiles were then averaged at each location, y, measured from the centre of gravity. The "absolute" mean concentration profile was constructed by merely averaging the individual concentration profiles in the absolute coordinate system.

Properties of Mean Concentration Profiles

Experimental data from continuous dye plumes in coastal currents have been extensively used to study "relative" diffusion, neglecting the random movements of the centre of gravity. For example, the statistical properties of "relative" mean concentration distributions in the wake of continuously diffusing dye plumes in coastal currents are known fairly accurately both from theoretical (Okubo and Karweit, 1969) and experimental (Murthy and Csanady, 1971; Bowden *et al.*, 1974; and Sullivan, 1971) studies. "Relative" mean concentration profiles have been approximated to be Gaussian with some theoretical justification (Fig. 11). However, quite often the cross-plume "relative" mean concentration distributions constructed from repeated observations exhibit skewness with depth and with distance from the source, presumably as a result of current shear in the horizontal and vertical directions. Gaussian approximation is therefore an exception rather than a rule in steady and uniform currents (Murthy and Csanady, 1971; Murthy, 1972).

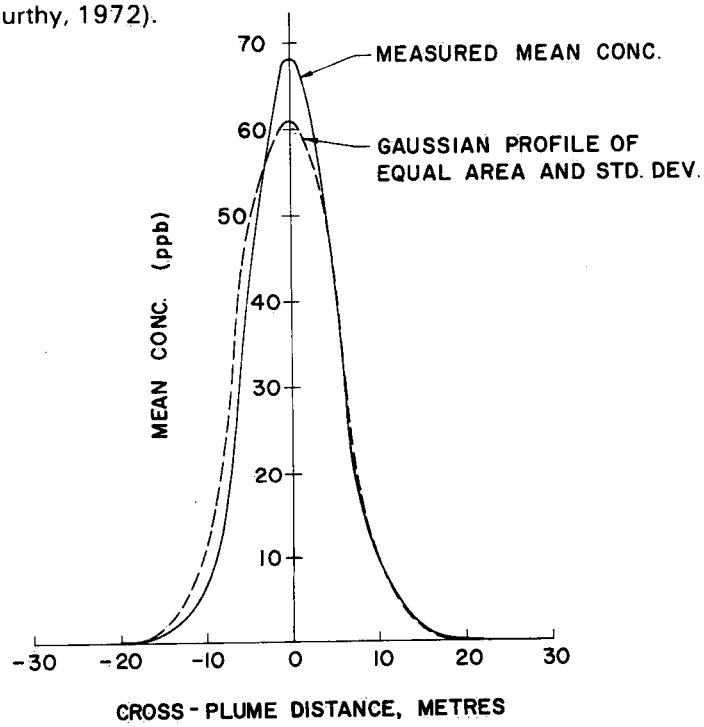

Figure 11. "Relative" mean concentration profile compared with equivalent Gaussian profile.

The above discussion has been concerned with the relative diffusion of the dye plume about its centre of gravity, neglecting the random movements of the centre of gravity ("meandering"). In reality, "meandering" is a dominant diffusion mechanism caused by turbulent eddies typically comparable to or larger than the plume itself. The net effect of meandering is to shear the mean

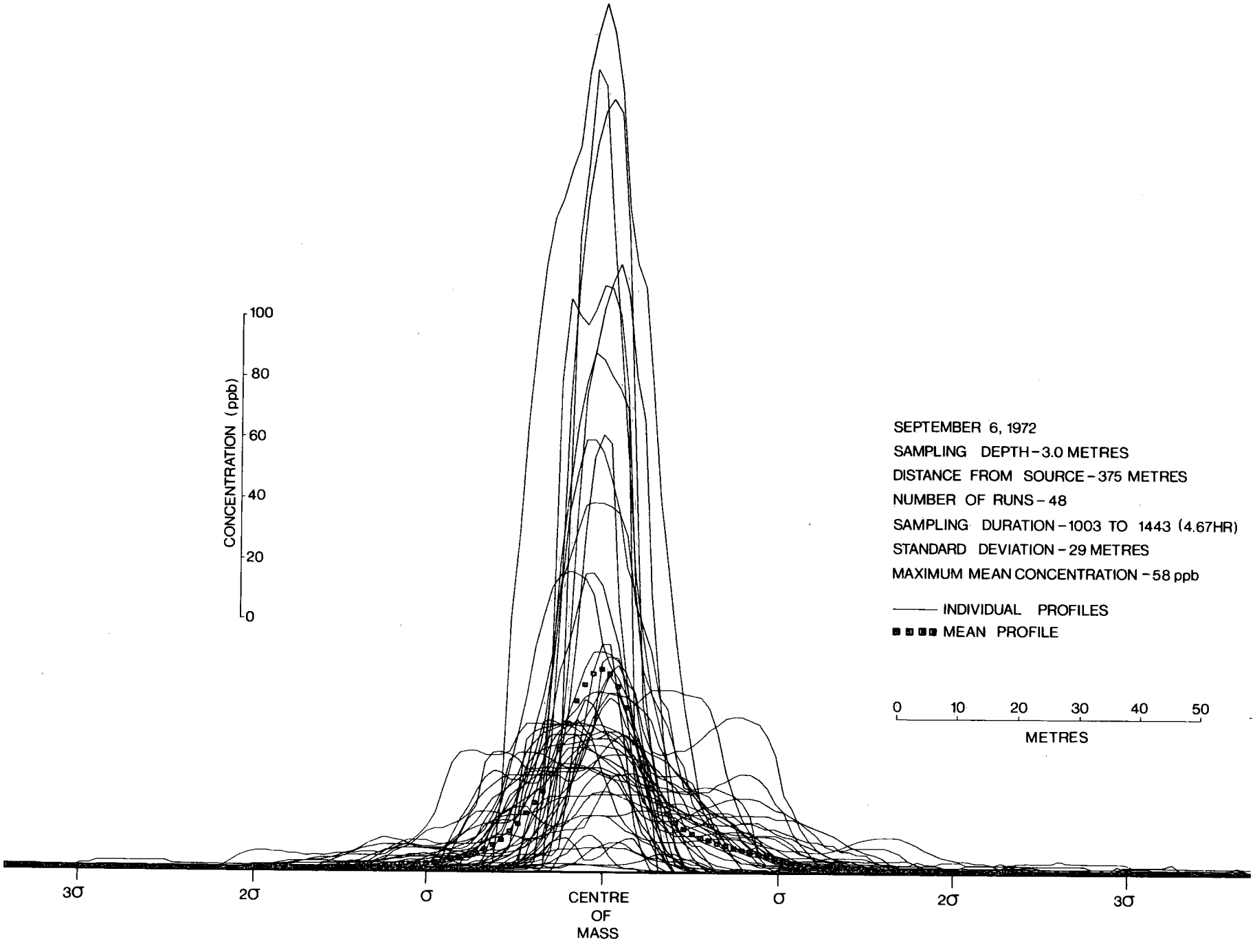

Figure 12. Cross-plume concentration distribution, relative.

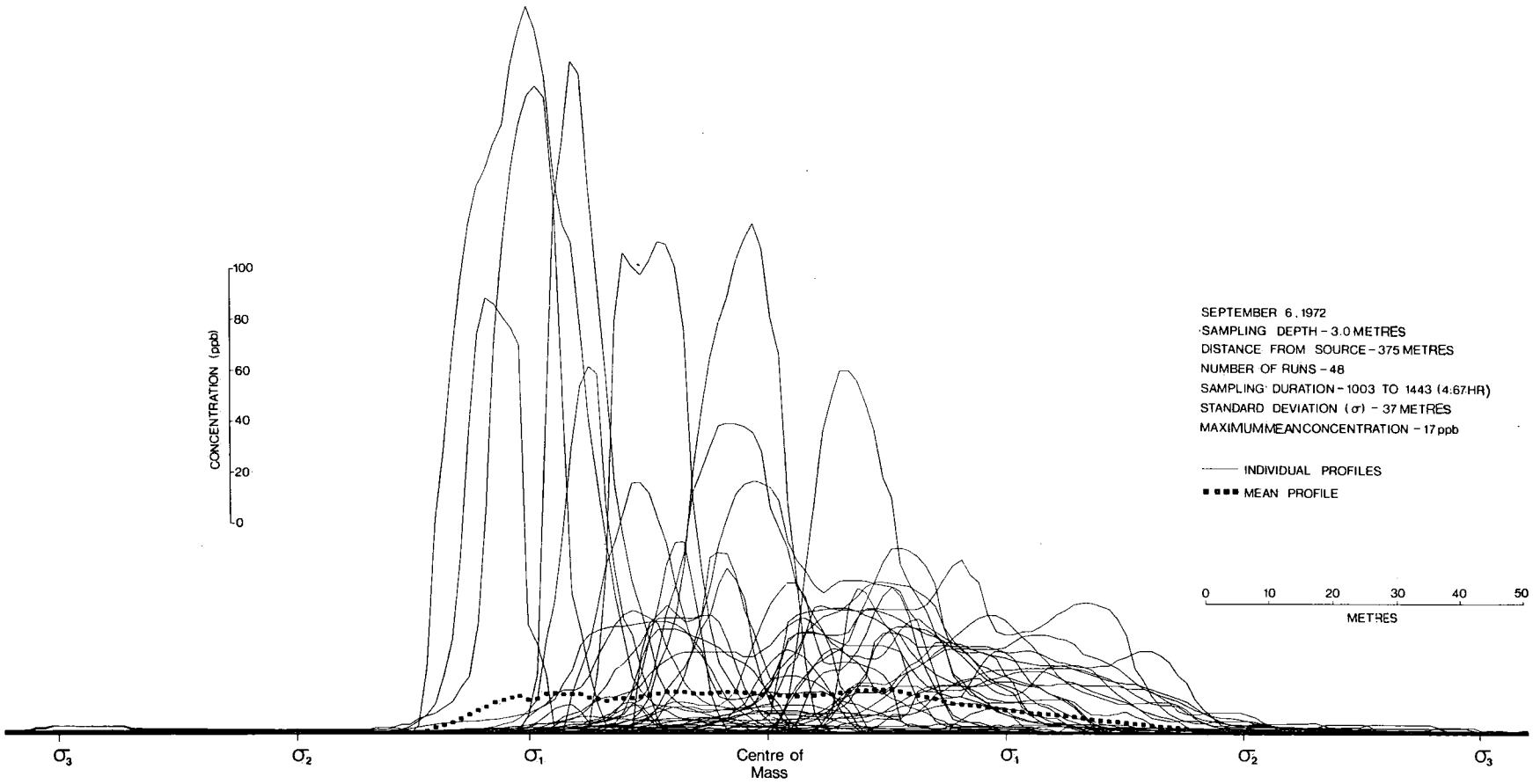

Figure 13. Cross-plume concentration distribution, absolute.

concentration profile. We will attempt to delineate the differences between "relative" and "absolute" mean concentration distributions constructed from a large number of cross-plume instantaneous concentration profiles obtained from a carefully conducted experiment during the International Field Year for the Great Lakes in coastal waters of Lake Ontario, off Oshawa (30 mi east of Toronto).

Figures 12 and 13 show the individual concentration profiles from 48 crossings at 3 m depth and at 375 m from dye source plotted against cross-plume distance y perpendicular to the mean axis of the plume. The individual profiles showed pronounced variability. The "relative" and "absolute" mean concentration profiles constructed from the 48 profiles are also shown. It is of interest to note the differences in the spread (as measured by some factor of standard deviation) and centre line concentration of the two profiles. The spread of the plume in absolute diffusion is greater than in the case of relative diffusion. The centre-line concentration is correspondingly less in relative diffusion than in the absolute diffusion.

In "relative" diffusion the size of the "patch" or "plume" sets a clear limit to the eddy size, and the effect of sampling time on the growth of the variance (or its square root, the standard deviation) is not a problem. However, the sampling time has considerable effect on the growth of the variance of meandering. Csanady (1963) has shown that the variance of meandering at a fixed distance of 750 m from dye source increases with sampling time before attaining a constant value in about 3 hr. The above arguments lead to the conclusion that the sampling-time effects are particularly important in "absolute" diffusion, where the combined effects of "relative" diffusion as well as "meandering" are responsible for concentrations observed at fixed points.

Properties of Concentration Fluctuation Profiles

While a great deal is known about the properties of the mean concentration profiles, very little is known about the properties of concentration fluctuations. In this section, some experimental data on the properties of concentration fluctuations in the wake of a continuous point source in coastal currents are discussed.

A statistical quantity which is used as a measure of the magnitude of concentration fluctuations is the variance or the mean square fluctuations (msf). The msf can be calculated from the observed individual profiles C(y) and their mean $\overline{C}(y)$,

$$\overline{C}^{12}(y) = \overline{|C(y) - \overline{C}(y)|^2}$$

A convenient non-dimensional parameter in characterizing fluctuations is the "relative intensity" of fluctuations, defined as the ratio of the root mean square (rms) to the local mean:

$$i_c(y) = |\overline{C}^{12}(y)|^{1/2} / \overline{C}(y).$$

Figures 14 and 15 show typical distribution of $i_c(y)$ from detailed experiments carried out in coastal currents of Lake Ontario. The cross-plume distance is normalized with S_y, the standard deviation of the mean concentration distribution $\overline{C}(y)$ (a measure of the horizontal length scale). The centre value $i_c(o)$ is an important parameter and of practical interest. In Table 1 a summary of $i_c(o)$ from several experiments is given. Such wide variation of the intensity of concentration fluctuations, from experiment to experiment, is attributed to day-to-day variation in turbulence level in coastal currents. The centre value $i_c(o)$ varied from as low as 0.1 to as high as 1.0, and near the edges of the plume it was still higher, of the order of 3 to 5. Such high ratios of rms to mean indicate that the concentration fluctuations are comparable in magnitude to the mean concentration, unlike velocity fluctuations.

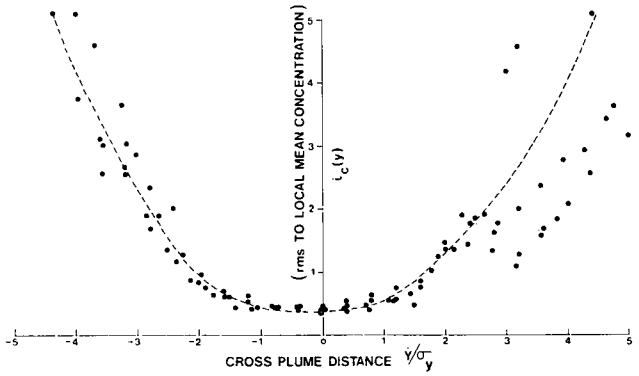

Figure 14. Concentration fluctuation profile.

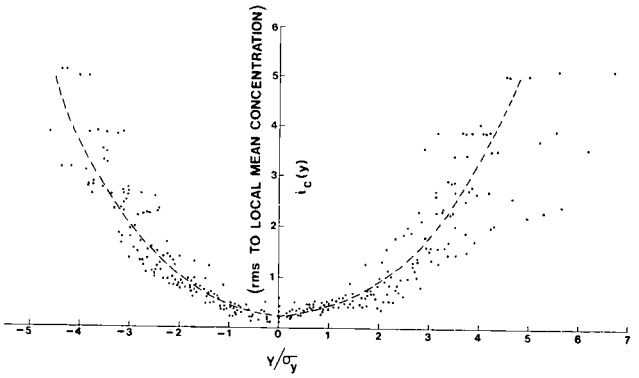

Figure 15. Concentration fluctuation profile.

Table 1. Observed Mean Values of $i_c(o)$ from Different Experiments

Experiment	$i_c(o)$	Remarks
June 6, 1968	0.30	Coastal zone, Lake Huron
Aug. 11, 1968	0.80	Niagara River mouth, Lake Ontario
Aug. 12, 1968	0.60	" " " " "
Aug. 13, 1968	0.55	" " " " "
Aug. 24, 1968	0.35	" " " " "
Aug. 28, 1968	0.40	" " " " "
June 4, 1969	0.80	Coastal zone, Lake Ontario
June 9, 1969	1.00	" " " "
June 11, 1969	0.30	" " " "
June 18, 1969	0.10	" " " "

Csanady (1967) and Juhat (1969), by solving a balance equation for msf, predict quasi-self-similar cross-plume $i_c(y)$ profiles, with centre value $i_c(o)$ being a floating parameter. Asymptotically this analysis yields $i_c(o) \sim 0.7$. Their theoretical results are qualitatively correct insofar as to predict the shape of self-similar cross-plume $i_c(y)$ profiles.

From a practical point of view, the mean concentration distribution $\overline{C}(y)$ is only a good predictor of observable concentrations (particularly the maximum concentration) if $i_c(y)$ is small. Near the centre, with $i_c(y)$ 1, the mean distribution is a fair-to-good predictor of observable maximum. Near the edges of the plume, it is entirely useless, since $i_c(y) > 1$.

Determination of Diffusion Characteristics

It is often difficult to interpret meaningfully the diffusion data and results from field experiments obtained under complex environmental conditions. However, at least the gross physical factors influencing the diffusion processes can be elucidated by constructing certain basic diffusion diagrams. One such diagram conventionally used is a plot of the effective diffusivity versus a length scale of diffusion (meaning that eddies comparable to this size are most effective in the diffusion of the dye plume). The effective diffusivity K_y was calculated by a simple formula, $K_y = S_y^2/2T$, where S_y, the standard deviation of the observed mean concentration distribution $\overline{C}(y)$, is determined by

$$S_y^2 = \frac{1}{q} \int_{-\infty}^{\infty} y^2 \, \overline{C}(y) \, dy,$$

and

$$q = \int_{-\infty}^{\infty} \overline{C}(y) \, dy$$

is the total amount of the dye at the depth of sampling, and T is the effective diffusion time approximated by X/U, where U and X are the mean current and the distance from the dye source, respectively. One can arbitrarily set a length scale of diffusion $L_y = 3S_y$, assuming that the measured mean concentration distributions are Gaussian. A logarithmic plot of the eddy diffusivity K_y and the length scale of diffusion L_y, for data from several diffusion experiments in coastal waters of lakes Erie, Ontario and Huron, is shown in Figure 16.

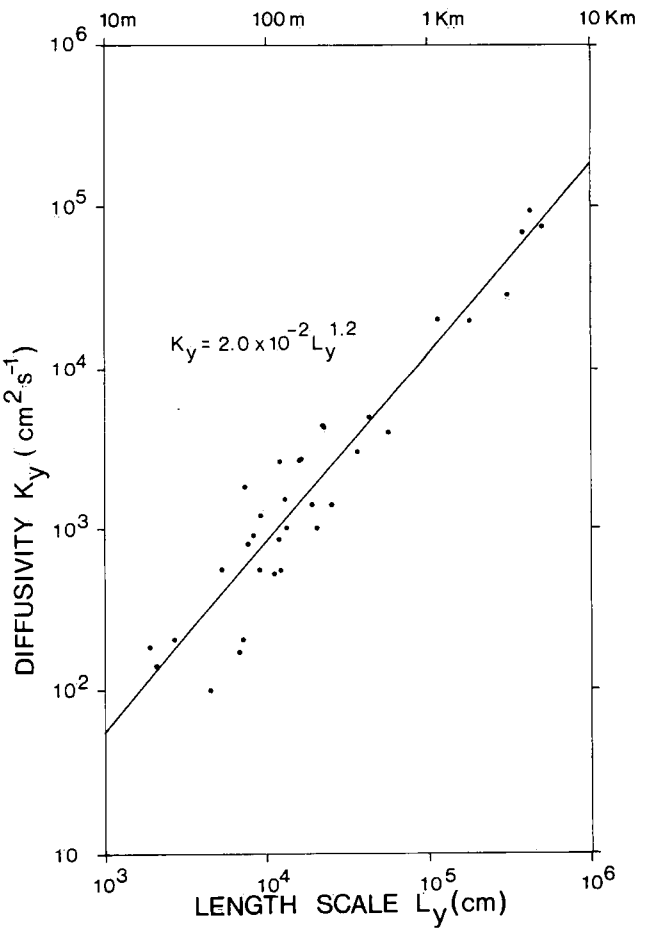

Figure 16. Horizontal eddy diffusivity vs length scale of diffusion.

A least square analysis of the data yields the following empirical relationship:

$$K_y = 2.0 \times 10^{-2} L_y^{1.2}.$$

A diffusion diagram of this type is quite useful for modeling coastal diffusion problems such as diffusion of effluent sewage of outfalls.

Large-Scale Diffusion Studies

EXPERIMENTAL METHODS

Instantaneous fluorescent "dye patches" are convenient experimental targets to study large-scale diffusion processes in natural bodies of water such as the Great Lakes. The experimental method consisted of generating a "dye patch" at selected depths by instantaneous release of a slug of Rhodamine B dye solution and following the subsequent diffusion of the dye patch as the lake currents and their eddies caused it to spread and dilute. The density of Rhodamine B dye solution was adjusted to the in situ density by adding methanol and surface water. Water samples taken at selected depths of dye injection were used to determine the in situ density. No attempt was made to adjust the temperature of the dye solution to the in situ temperature, and usually the initial mixing during the injection was sufficient to compensate for the temperature difference. The methods of dye release and the fluorometric sampling of the diffusing patch have been discussed earlier.

Generally, the dye release, which constitutes the beginning of the experiment, took place in the early hours of the day. The early stages of diffusion are difficult to sample since the dye patch has small areal extent and high concentrations beyond the measurability range of the fluorometers. Moreover, any significant disturbance of the patch by the sampling vessel could alter the dispersion characteristics considerably. The dye patch was sampled using ship borne fluorometers by a carefully chosen network of crossings across the patch. Launch-based operation was used for sampling when the diffusing patch was small (say, hundreds of metres). When the diffusing patch had grown to the size of a few kilometres, a ship was used for sampling the dye patch. To obtain as rapid (quasi-synoptic) and accurate measurement of the diffusing patch as possible, the sampling procedure was discussed with the crew of the sampling vessels. Their experience, particularly in the area of navigation, was no doubt very valuable. Besides, precision navigation of the sampling boats, accurate bookkeeping of all sampling courses, speeds and times are necessary for proper synthesis of the data. This, to a large extent, was provided by the crews of the sampling vessels involved.

When the dye patch was small, during the initial stages of diffusion, the positions of the sampling launches were fixed relative to the anchored mother ship. The positions were marked at the beginning of the crossing and at the end, when the fluorometer reading had dropped to zero or a very low value compared with the peak in that crossing. During later stages of diffusion when the ship was used for sampling, direct fixing of position on charts by using the log reading and the compass course was used.

Large-scale diffusion experiments were carried out in the general vicinity of a network of meteorological and current meter moorings to take advantage of the general environmental data to interpret diffusion data and results.

Experiments covered time scales ranging from 3 to 80 hr and the corresponding spatial scales ranged from 0.1 to 15 km in the horizontal and up to 6 m in the vertical.

DATA ANALYSIS

The horizontal scales of motions in the lakes and oceans are much greater than the vertical scales and, therefore, in many cases, their effect on mixing may be considered separately. This idea has been explored by a number of investigators with considerable success. In this approach, it is assumed that the introduced substance is subject to horizontal mixing within a sufficiently thin homogeneous layer so that all variations in both concentration and velocity may be neglected. However, the importance of vertical diffusion cannot be neglected even though the diffusing contaminant is, for practical purposes, confined to a very thin layer. The combined action of vertical shear in the horizontal mean current and vertical diffusion may produce considerable effective horizontal diffusion.

Horizontal distributions of dye concentration were prepared for each experiment from a good coverage of the dye patch during a reasonable sampling time interval and thus they could be treated as quasi-synoptic. The diffusion time is taken from the time of dye release to the

middle of the time interval chosen for observing the horizontal distributions. The horizontal dye distributions are generally relative to a drogue (released with the dye) in a system moving with the mean current. It is usually not necessary to correct for translation during the sampling interval, since the analysis of the data is carried out in a moving frame of reference (relative diffusion).

Typical horizontal concentration distributions constructed as lines of equal concentration are shown in Figure 17 from a carefully conducted experiment in Lake Ontario. The starting point in the analysis of field diffusion data is the calculation of the variances from the measured spatial concentration distributions of the dye patch. Often the measured concentration distributions are converted to equivalent radial symmetric distributions from which variances are calculated. It is implicit in such an analysis that the diffusion of the dye patch is governed by two-dimensional homogeneous turbulence.

The measured spatial concentration distributions are converted into equivalent radially symmetric distributions by defining the radius of a circle, $r = (A_c/\pi)^{1/2}$, as a measure of the area A_c enclosed by a particular concentration contour C. Then the concentration distribution C(r, t), characterized by the equivalent radii r and diffusion time t (i.e., time elapsed since dye release) would represent approximately the equivalent radially symmetric distribution. The variance $S_r^2(t)$ corresponding to the radially symmetric distribution C(r, t) is given by

$$S_r^2(t) = \int_0^\infty r^2\, C(r, t)\, 2\pi r\, dr \Big/ \int_0^\infty C(r, t)\, 2\pi r\, dr. \quad (1)$$

The elongated appearance of the dye patch and the asymmetry in the observed concentration distributions do not support the radially symmetric hypothesis. Anisotropic turbulence (i.e., turbulent eddies which are more intense in the direction of the mean flow than across it) combined with "shear diffusion" due to vertical shear in the horizontal mean current, gives rise to enhanced mixing in the longitudinal direction. With these observed features in mind, the variances were computed by direct integration of the observed concentration distributions. If we choose a convenient rectangular coordinate system through the centre of the distribution, with the x-axis in the direction of the mean current, the appropriate variances corresponding to a two-dimensional concentration distribution C(x, y, t) are defined as follows.

$$\text{Longitudinal: } S_x^2(t) = \frac{1}{Q}\int_{-\infty}^{\infty}\int x^2\, C(x, y, t)\, dx\, dy \quad (2)$$

$$\text{Transverse: } S_y^2(t) = \frac{1}{Q}\int_{-\infty}^{\infty}\int y^2\, C(x, y, t)\, dx\, dy \quad (3)$$

where $Q = \int_{-\infty}^{\infty}\int C(x, y, t)\, dx\, dy$

DIFFUSION CHARACTERISTICS

Horizontal

It is customary to interpret diffusion data and results from field experiments by constructing certain basic diffusion characteristics (Stommel, 1949; Okubo, 1971). Two commonly used diffusion characteristics are the variance of the horizontal concentration distribution of the diffusing substance versus the length scale of diffusion. A log-log plot of the variance against time determines a straight line, which provides the empirical law

$$S^2 = at^m. \quad (4)$$

Assuming that the concentration distribution within the patch is isotropic, we can define an apparent diffusivity

$$K = \tfrac{1}{2}(dS^2/dt). \quad (5)$$

Eliminating t from Equations 4 and 5 yields

$$K = cS^n \quad (6)$$

where

$$c = (m/2)\, a^{1/m} \text{ and } n = 2(m-1)/m$$

Combining Equations 4 and 6, some familiar theoretical diffusion characteristics can be deduced. From physical reasoning and dimensional considerations, m should be an integer. If $m = 1$, then the variance grows linearly with the diffusion time scale, which corresponds to the Fickian diffusion model with a constant diffusivity. If $m = 2$, then the variance grows as the square of the time scale, which corresponds to the shear diffusion model with a linear dependence of eddy diffusivity on length scale. If $m = 3$, then the variance grows as the cube of the time scale, corresponding to the inertial subrange diffusion with the familiar Richardson's "four-thirds" power law dependence of eddy diffusivity on the length scale. These diffusion laws are summarized in the table on page 23.

With this simple theoretical framework, we will present diffusion characteristics constructed from experimental data. Figure 18 shows the log-log plots of variance as a function of the diffusion time scale.

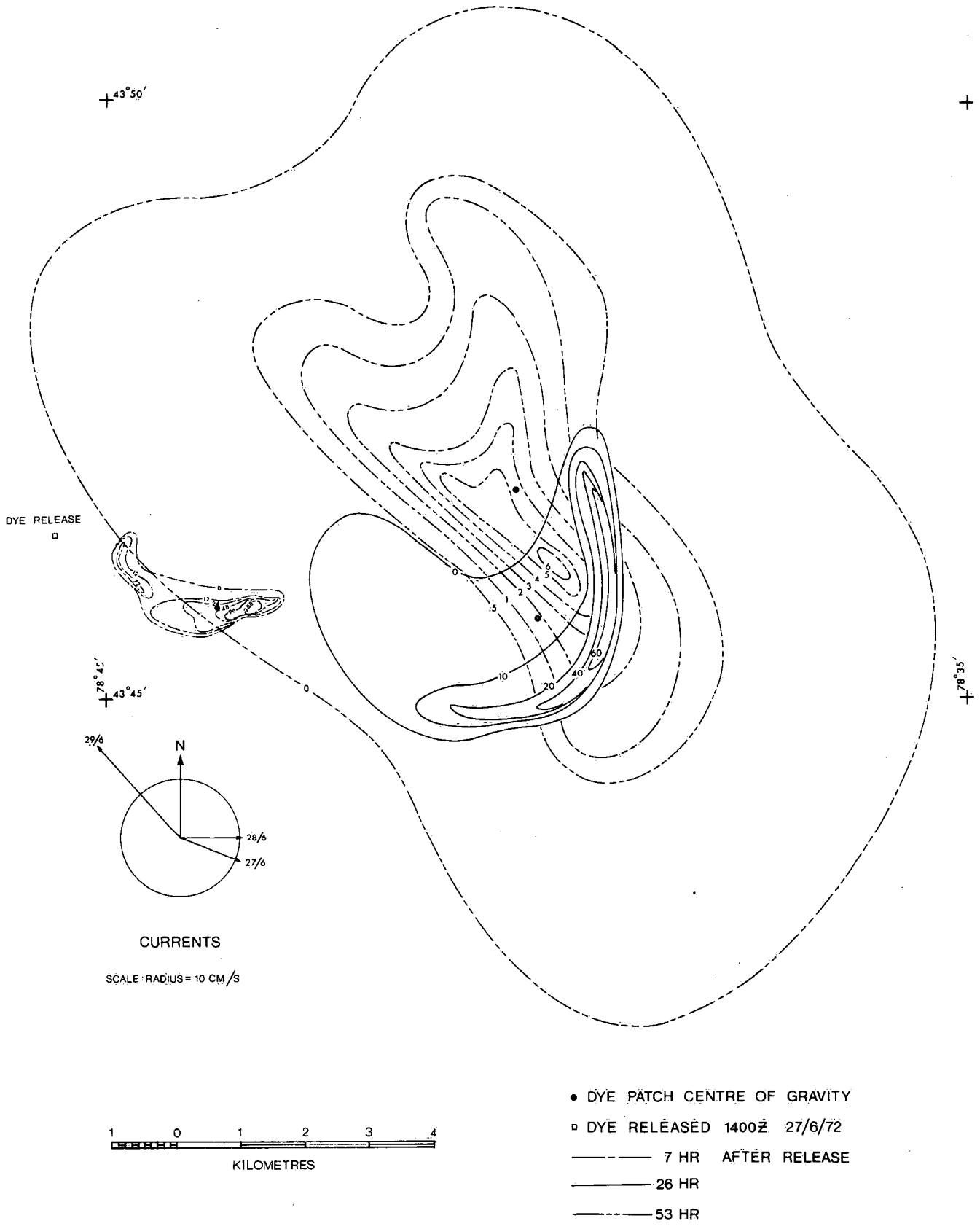

Figure 17. Quasi-synoptic horizontal distribution of dye concentration (ppb).

m	n	Diffusion law	Diffusion parameters	Diffusion model
1	0	K = const.	Const. diffusivity	Fickian diffusion
2	1	$K \sim q\,L$	q diffusion velocity L length scale	Shear diffusion
3	4/3	$K \sim \epsilon^{1/3} L^{4/3}$	ϵ energy dissipation rate L length scale	Inertial subrange diffusion

Regression equations defining the coefficient a and the exponent m in Equation 4 are also given in Figure 18. The exponent m lies between 2 and 3, ruling out the Fickian diffusion model. The eddy diffusivities were calculated using the corresponding values of a and m from Equation 6.

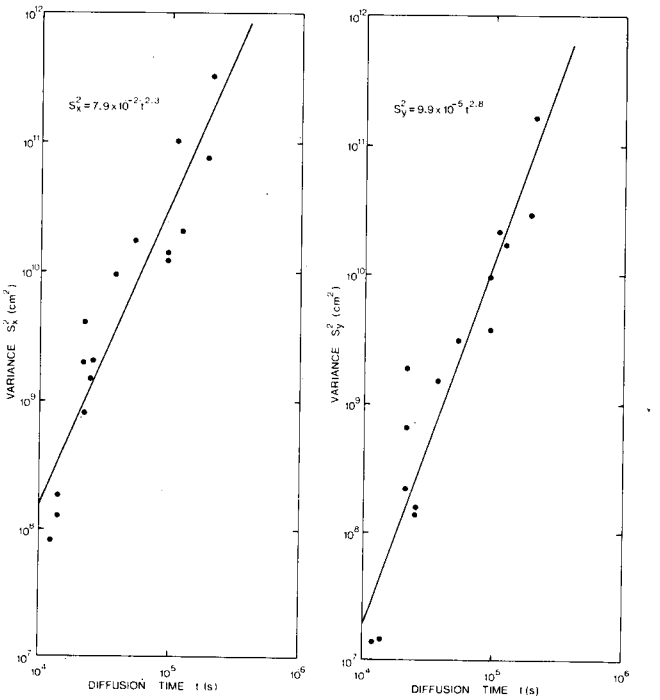

Figure 18. Horizontal variance vs diffusion time scale.

The standard deviation S of the horizontal concentration distribution is a good measure of the length scale of diffusion (meaning that turbulent eddies of the size comparable to S are most effective in the diffusion of the dye patch). However, to be compatible with the published oceanic literature, we will define the length scale as *three* times the standard deviation of the observed concentration distribution. Figures 19 and 20 show logarithmic plots of eddy diffusivity as a function of the corresponding length scale. Regression equations defining the coefficient C and the exponent n in Equation 6 are also given in the figures.

Since the exponent m in Equation 4 lies between 2 and 3 and is not explicitly defined, the exponent n in Equation 6 is not clearly defined in accordance with any theoretical model.

As pointed out earlier, a wide spectrum of horizontal motions exists in the lakes. Thus, the horizontal eddy diffusivity usually increases with the scale of mixing considered. As expected, however, the deep water values are gradually one to two orders of magnitude smaller than those of the surface layer values. A plausible explanation for the smaller values at greater depths could be that the

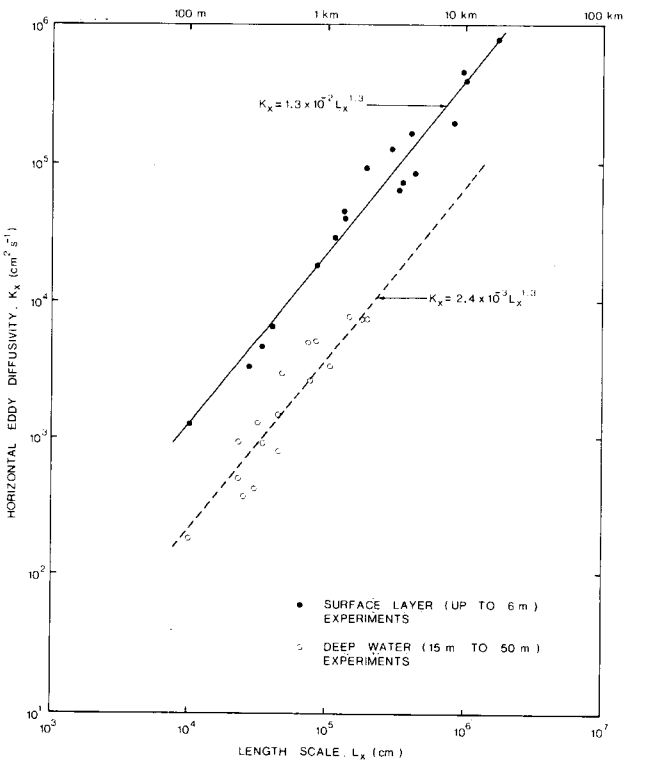

Figure 19. Horizontal (longitudinal) eddy diffusivity vs diffusion length scale.

available turbulent kinetic energy for diffusion decreases with depth.

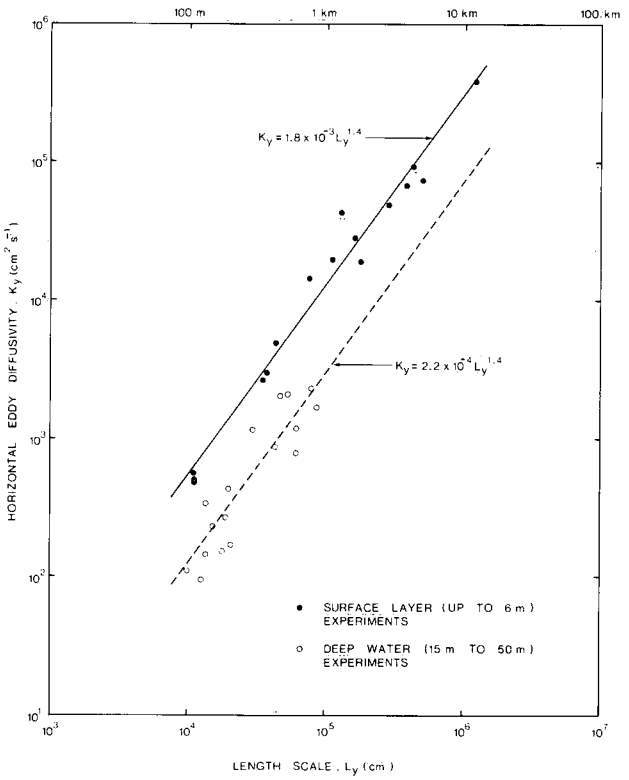

Figure 20. Horizontal (lateral) eddy diffusivity vs diffusion length scale.

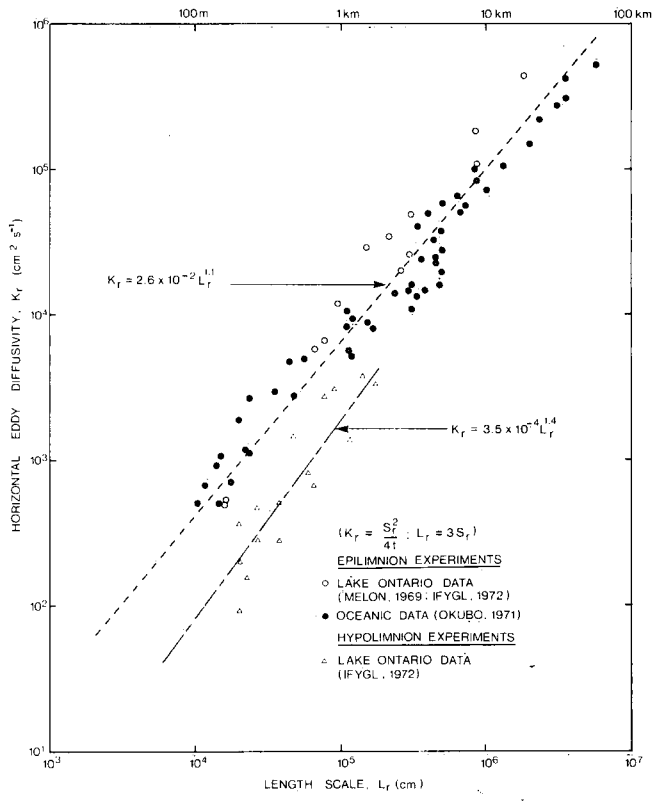

Figure 21. Comparison of oceanic diffusion data with Great Lakes diffusion data (MELON (Massive Effort on Lake Ontario), 1969, and IFYGL (International Field Year for the Great Lakes), 1972: unpublished data).

It may be of interest to compare the present data with oceanic data summarized by Okubo (1971). Figure 21 shows such a comparison, and considering that the experiments were conducted in a wide variety of environmental conditions, the lake data compare favourably with the oceanic data. This would imply that the diffusion rate in the lake is approximately the same as that of oceans.

An important conclusion that can be drawn from the experimental results is that the horizontal eddy diffusivity grows faster than given by the Fickian model and somewhat slower than in the "inertial subrange". Although these diffusion characteristics cannot be justified entirely from theoretical arguments, they could be viewed as a parameterization, since they have been constructed from experimental data obtained in widely varying environmental conditions. The dependence of the horizontal eddy diffusivity on the length scale provides useful guidelines for modeling of practical diffusion problems.

Vertical

In contrast to the horizontal diffusion, the process of vertical diffusion is controlled primarily by small-scale motions characteristic of a stably stratified water column. In addition, wind mixing plays an important role in providing turbulent energy to the epilimnion and possibly down to the thermocline. Unlike the horizontal eddy diffusivity, the vertical diffusivity does not depend uniquely on the scale of diffusion. Efforts have been directed to relate the vertical diffusivity to the environmental factors relevant to vertical mixing.

Kullenberg (1969) found empirically that K_z could be related to the stratification of water, current shear, and wind speed (to be specific, wind stress); he proposed a dimensionally correct formula:

$$K_z = c\,\overline{W}^2\,\overline{N}^{-2}\left|\overline{dq/dz}\right| \qquad (7)$$

where c is a numerical constant, W^2 is a measure of the wind stress at the surface, N is the Brunt Vaïsala

frequency defined by $\overline{N}^2 = (g/\overline{\rho})(d\overline{\rho}/dz)$ and $\overline{dq}/dz$ is the absolute value of the mean current shear. Later, Kullenberg *et al.* (1973), summarizing data obtained from Lake Ontario, found that for persisting winds greater than 5 m/s, the vertical mixing in the upper zone could be expressed as

$$K_z = (8)\, 10^{-8}\, \overline{W}^2\, (\overline{N}^2)^{-1} |\overline{dq}/dz| \qquad (8)$$

where W^2, N^2, and $|dq/dz|$ are the mean square of the wind speed, the mean Brunt Vaisala frequency, and the mean current shear, respectively.

For low and varying winds, vertical internal mixing is governed by local processes. The energy source is then the kinetic energy of fluctuations. In a later paper, Kullenberg *et al.* (1974) proposed the following relation for weak local winds.

$$K_z = 4.1 \times 10^{-4}\, \overline{q'^2}\, (\overline{N}^2)^{-1} |dq/dz| \qquad (9)$$

where $\overline{q'^2} = \overline{u'^2} + \overline{v'^2}$: the kinetic energy of current fluctuations. Presumably, this relation may also be applicable to the deeper layer below the thermocline. Figures 22 and 23 show the empirical vertical diffusion characteristics corresponding to Equations 8 and 9 and they can be used as guidelines in numerical calculations of dispersion in practice.

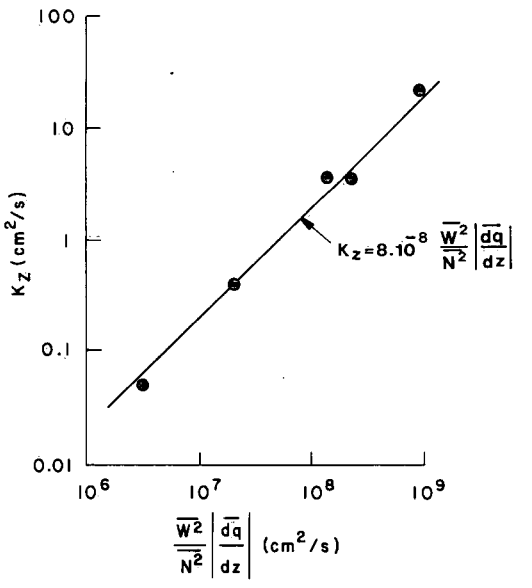

Figure 22. Vertical eddy diffusivity vs wind stress, stability parameter and current shear.

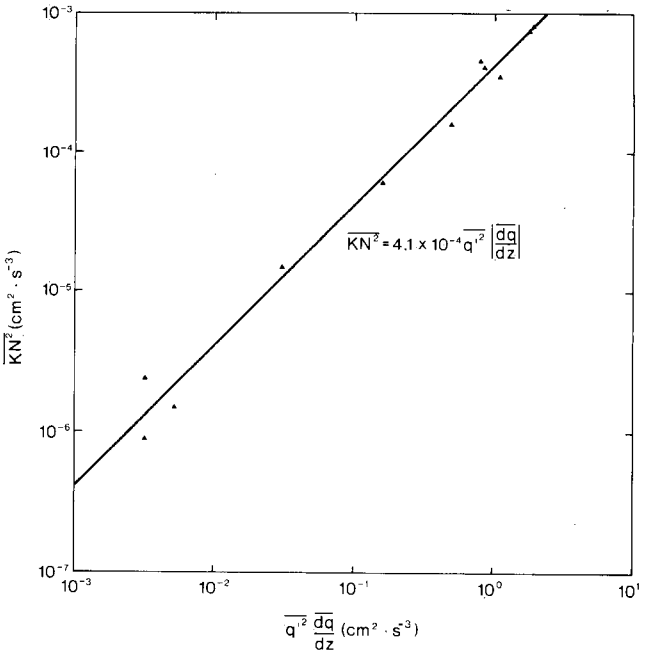

Figure 23. Vertical eddy diffusivity vs stability parameter, turbulent kinetic energy and current shear.

REFERENCES

Bowden, K.F., Krauel, D.P. and Lewis, R.E., 1974. Some features of turbulent diffusion from a continuous source at sea. Adv. Geophys., Vol. 18A, 315-329.

Cederwall, K. and Hansen, J., 1968. Tracer studies on dilution and residence time distribution in receiving waters. Water Res., Vol. 2, 397-410.

Csanady, G.T., 1963. Turbulent diffusion in Lake Huron. J. Fluid Mech., Vol. 17, 360-384.

Csanady, G.T., 1967. Concentration fluctuation in turbulent diffusion. J. Atmos. Sci., Vol. 24, 21-28.

Gifford, F.A., 1959. Statistical properties of a fluctuating plume dispersion model. Adv. Geophys., Vol. 6, 117-137.

Gifford, F.A., 1960. Peak to average concentration ratios according to a fluctuating plume dispersion model. Int. J. Air Pollut., Vol. 3, 253-260.

Juhat, M.K., 1969. The transformation of probability characteristics of concentration of scalar passive substances in marine environment. Ph.D. thesis, Academy of Sciences, U.S.S.R. Institute of Oceanology, Moscow (in Russian).

Kullenberg, G., 1969. Measurements of horizontal and vertical diffusion in coastal waters. Acta Regiae Soc. Sci. Litt. Gothob., Geophys. 2, Goteborg, 52 p.

Kullenberg, G., Murthy, C.R. and Westerberg, H., 1973. An experimental study of diffusion characteristics in the thermocline and hypolimnion regions of Lake Ontario. Proc. 16th Conf. Great Lakes Res., Int. Assoc. Great Lakes Res., pp. 774-790.

Kullenberg, G., Murthy, C.R. and Westerberg, H., 1974. Vertical mixing characteristics in the thermocline and hypolimnion regions of Lake Ontario. Proc. 17th Conf. Great Lakes Res., Int. Assoc. Great Lakes Res., pp. 425-434.

Murthy, C.R., 1972. Complex diffusion processes in coastal currents of a lake. J. Phys. Oceanogr., Vol. 2, 80-90.

Murthy, C.R. and Csanady, G.T., 1971. Experimental studies of relative diffusion in Lake Huron. J. Phys. Oceanogr., Vol. 1, 17-24.

Okubo, A., 1971. Oceanic diffusion diagrams. Deep-Sea Res., Vol. 18, pp. 789-802.

Okubo, A. and Karweit, M.J., 1969. Diffusion from a continuous source in uniform shear flow. Limnol. Oceanogr., Vol. 14, 514-520.

Stommel, H., 1949. Horizontal diffusion due to oceanic turbulence. J. Mar. Res., Vol. 8, pp. 199-225.

Sullivan, P.J., 1971. Some data on the distance-neighbour function for relative diffusion. J. Fluid Mech., Vol. 47, pp. 601-607.

Fluorometer Calibration

Introduction

The accurate determination of quantitative relationships between instrument output and sample concentration is somewhat more difficult for high-volume continuous-flow fluorometers than for laboratory instruments equipped to process samples contained in small cuvettes. A system was devised whereby eight Turner model III fluorometers and a Zone Research in situ fluorometer were calibrated for continuous flow operation at 16 different concentration levels of rhodamine between 1×10^{-10} and 4×10^{-7}.

To cover such a broad concentration range, nine sensitivity ranges were created for the Turner instruments by using combinations of zero to two each 50% and 10% neutral density filters over the secondary colour filter with the built-in range aperture set for maximum sensitivity.

The Zone Research instrument was equipped to measure concentrations from about 1×10^{-10} to 2×10^{-7}, with response proportional to the log of the concentration over a single range.

The actual calibration system consisted of a sample reservoir, pump, and all of the fluorometers, coupled together in series, creating a closed circuit. The dye concentration in the circuit could be raised by adding solution to the reservoir, where baffles over the sample return caused sufficient turbulence to bring the concentration in the system to a new equilibrium quickly.

Procedure

The system was charged with an accurately measured volume of distilled water. The instruments and pump were run for about an hour to purge all air and achieve thermal and electrical stability. Initial readings were taken, and calibration continued with the stepwise addition of solutions of known concentration. With each addition, time was allowed for thorough mixing before the readings were taken.

Cumulative errors in the determination of amounts added were minimized by using an accurately calibrated burette as a metering device. Individual increments were obtained by subtracting the reading before the addition from the reading after it; however, for total amounts added, only initial and final volume readings were used. The concentration in the system was computed for each increment of solution added; and for each concentration level, instrument readings were taken with any of the nine filter ranges, producing on-scale results.

As the procedure progressed, the incremental additions were made from standard solutions of increasing concentration, such that the size of the increments added varied little throughout the calibration process.

Upon completion of the calibration, the data were used to prepare graphs showing instrument output plotted against concentration for each range where applicable. Graph sets for every instrument made possible complete reduction of field data to actual concentrations. Typical calibration graphs for Turner Model III fluorometer are shown in Figure 4.